Impact of Roughness on the Deformation and Adhesion of a Rough Metal and Smooth Mica in Contact

John M. Levins and T. Kyle Vanderlick*

Department Chemical Engineering, University of Pennsylvania, Philadelphia, Pennsylvania 19104-6393

Received: August 22, 1994; In Final Form: November 23, 1994[⊗]

We investigate the impact of microscopic roughness on the adhesion and deformation of a rough metal and molecularly smooth mica in contact. Silver and gold films, prepared by thermal evaporation, were brought into contact with mica using the surface forces apparatus; multiple beam interferometry was used to characterize, *in situ*, both surface deformations and the roughness of the ensuing metal/mica interface. As a basis for comparison, we also present measurements for mica/mica contact. We find that on bringing the metal films into contact with mica, their roughness decreases over time, and concurrently the area of flattened metal/mica contact increases. We measured the adhesion force between mica and metals having different degrees of roughness, and found that adhesive forces are not extinguished until the roughness is greater than about 10 nm. This behavior, as well as the general irreversibility of the adhesion process, indicate that the metal films are undergoing significant plastic deformations.

I. Introduction

Adhesion between solid bodies is important to many areas of science and technology, including lubrication, the processing and handling of powders and particulates, and the manufacture and operation of mechanical devices and components. Simply stated, the phenomenon of adhesion occurs when two solid bodies are brought sufficiently close that attractive intermolecular forces acting between their surfaces cause them to stick together.[1] These intermolecular forces can be of a variety of types, including van der Waals forces and covalent or metallic bonding forces,[2,3] but they are all short ranged; most extend out to only a few nanometers or less. In practice it is often difficult to get two solids this close together so they adhere. One primary reason for this is that all solid surfaces, with few exceptions, are rough, and roughness reduces adhesion by limiting the area over which two surfaces can approach to within the range of intermolecular forces.[1,4,5]

The few fundamental investigations of adhesion that have been performed to date have avoided complications caused by surface roughness. This has been accomplished by using either materials of low elastic modulus, which could deform about asperities to attain intimate solid/solid contact, or by working deliberately with molecular smooth surfaces.

One of the most important investigations was carried out in 1971 by Johnson, Kendall, and Roberts (commonly referred to as JKR) who measured the adhesion and deformation of soft rubber spheres in contact.[6] Although their rubber surfaces were rough, on the order of 20 nm, they found that adhesion occurred on contact, requiring a finite force to separate them. Furthermore, they found that the surfaces deformed on contact, resulting in a finite area of flat rubber/rubber contact; application of a positive load increased the area. JKR developed a theory to predict the adhesion force and the degree of deformation, and their experimental results agreed very well with prediction. The basis of the theory, which assumed that the rubber was smooth and perfectly elastic, was the assumption that adhesion forces were of such short range that they operated only within the deformed area where contact between the rubbers was intimate.

Others have performed similar experiments since then;[7,8] most notably, Chaudhury and co-workers recently used a novel technique to systematically modify the surface free energy of lenses of poly(dimethylsiloxane).[9,10] They have found that JKR theory predicts the adhesion and deformation of fairly smooth soft elastic solids reasonably well, but not perfectly. For example, hysteresis in loading−unloading cycles has been observed for fluorinated surfaces.[9,11,12]

In the mid 1970's, the first detailed measurements of the adhesion between hard, molecularly smooth materials were obtained. These measurements were made using the surface forces apparatus (SFA), a device developed in 1969 by Tabor and Winterton[13] and later refined into its present form by Israelachvili.[14] The SFA allows direct measurement of the force acting between two molecularly smooth surfaces as a function of their separation, down to contact. One of the surfaces is mounted on a leaf spring which deflects in response to forces acting on it. The separation of the surfaces, shaped as cylinders and oriented at right angles, can be controlled to within angstroms; multiple beam interferometry is used to measure surface separation with the same, or nearly the same, resolution.

Using the SFA, Israelachvili, in his Ph.D. thesis, presented the first measurements of the adhesion and deformation of two molecularly smooth sheets of muscovite mica in contact.[4,15] The shape of the deformed surfaces was found to agree well with that predicted by JKR theory. These measurements were later continued in much greater detail by Horn, Israelchvili, and Pribac, who measured the deformation and adhesion as a function of applied load.[16] Again, reasonable agreement was found with JKR theory, and observed deviations were attributed to inelastic behavior of the glue supporting the mica sheets. More recently, Chen, Helm, and Israelachvili used the SFA to study the adhesion of mica surfaces coated with a variety of surfactants.[17] They found significant hysteresis in loading−unloading cycles for those cases where one or both of the surfactant layers was in an amorphous or fluid-like state; hysteresis was not observed if either surfactant layer was in a crystalline state. For those surfaces exhibiting hysteresis, they found the adhesive force increased over time of contact; after long times the adhesion agreed well with that predicted by JKR theory. These observations, along with those made by Chaudhury

* To whom correspondence should be addressed.
[⊗] Abstract published in *Advance ACS Abstracts,* March 15, 1995.

0022-3654/95/2099-5067$09.00/0

for polymer surfaces,[9,10] indicate that molecular-level mechanisms at the surface can play a role in governing adhesion. Simple adhesion models, such as that proposed by JKR, do not account for such mechanisms.

A few other surfaces besides mica have been employed in the SFA; however, all have been extremely smooth. Merrill *et al.* put sheets of poly(ethylene terephthalate) in the SFA and measured the adhesion between them, again obtaining good agreement with JKR theory.[8] More recently, Horn and co-workers have put smooth sheets of silica in the SFA and have observed significant charge transfer between mica and silica surfaces upon contact, leading to extremely strong adhesion.[18,19] They showed that charge transfer also occurs between a silica surface coated with an amine-terminated surfactant in contact with a bare silica surface.[20]

Despite all that we have learned from the investigations described above, we know very little regarding the influence of surface roughness on adhesion. In fact, most of our limited knowledge has come from investigations performed by Tabor and co-workers nearly 20 years ago.[4,21-23] One of the most informative of these studies was carried out by Fuller and Tabor,[21] who measured the adhesion of a nominally smooth rubber sphere to a rough sheet of Perspex. The roughness of the Perspex was increased by bead blasting, and a profilometer was used to characterize the topography. They found that the adhesive force dropped off with increasing roughness, becoming negligible at approximately 1 μm roughness. In addition, they found the rate at which adhesion decreased with roughness was steeper for harder rubbers. They modeled the rough surface as a distribution of asperities with varying heights, the tallest of which adhered to the smooth surface as predicted by JKR theory. Their analysis indicated that, for materials harder than rubber (such as ceramics), roughness of just a few nanometers would be sufficient to extinguish adhesion. Since their analysis was strictly valid only for purely elastic materials, they emphasized that this behavior would not hold for materials likely to exhibit plastic deformations, such as metals.

These predictions supported the earlier adhesion measurements of Gane, Pfaelzer, and Tabor.[24] They found that fairly smooth hard solids of high surface free energy, such as titanium carbide, glass, sapphire, diamond, and germanium, did not adhere; this was despite the fact that measurements were performed in ultrahigh vacuum and thus the surfaces were very clean. They speculated that the lack of adhesion was due to small scale roughness, on the order of a few nanometers. Unfortunately, they were not equipped to measure roughness on such a fine scale. In that same study, they observed strong adhesion between fairly hard, yet ductile materials such as gold and copper. They believed this was due to plastic deformation of the solid/solid junctions as they were being separated, thus suggesting that inelastic behavior can also play a significant role in the adhesion between solids. This observation has been supported by more recent experiments where a tungsten tip was pressed against a clean metal: significant plastic deformation was observed on separating the surfaces, resulting in strong adhesion.[25,26]

We recently used the SFA to measure the adhesion between mica and microscopically rough silver,[27] and found that the strength of adhesion increased irreversibly over time in contact. We attributed this dynamic behavior to a time-dependent decrease in the roughness of the silver surface caused by the action of attractive surface forces which compressed the mica against the silver. Unfortunately, we were unable to characterize the degree of roughness at the silver/mica interface, and thus our conclusions were only qualitative.

Clearly, fundamental investigations of the adhesion of rough surfaces require techniques that are capable of characterizing roughness, even on the order of angstroms, at a solid/solid interface *in situ*. Recently, we showed how such measurements can be obtained.[28] In our procedure, multiple beam interferometry is used to detect the presence of dielectric material trapped between the two solid bodies; measurements over localized areas (of order μm^2) spanning across the entire region of nominal contact are obtained simultaneously. The key to turning the raw interferometric data into quantitative information related to the structure and degree of surface roughness is to compare the light transmitted through the rough solid/solid interface to that through one which is smooth, i.e., where the contact is perfectly intimate. As we previously demonstrated,[28] and exploit herein, there are many situations for which it is not at all difficult to construct the latter.

The use of multiple beam interferometry in the application just described relies on capturing the spectrum of light transmitted through the surfaces quantitatively, locally (over areas as small as possible), and in full detail. Furthermore, the analysis and interpretation of the captured spectra is based on predictions using classical interference theory, taking into account the optical properties of all materials which comprise the given interference filter. Executed with these capabilities and under these conditions, we have termed the technique extended spectral analysis of multiple beam interferometry (ESA-MBI) and have given full account of the experimental details.[29] As stated previously, the surface forces apparatus relies on the application of multiple beam interferometry to monitor surface separation and associated deformations. Hence together, ESA-MBI and the SFA provide a very powerful method to study the impact of roughness on adhesion.

In this paper, we present ESA-MBI and SFA measurements of the deformation and adhesion of a microscopically rough metal in contact with molecularly smooth mica; the metals used were silver and gold. As a basis for comparison, we also present similar measurements for contact between two molecularly smooth mica surfaces. We show how nanometer-scale roughness of the metals impacts both adhesion and associated deformations. Evidence of inelastic behavior is also revealed by the structure of the interface and the time dependence of the adhesion process.

II. Background

A. Use of Multiple Beam Interferometry to Characterize Roughness and Deformations. We have previously described in detail how ESA-MBI can be used to characterize roughness at the interface between metal and mica in contact.[28] Here we will summarize the results of that study, with emphasis on those details relevant to this investigation.

Multiple beam interferometry requires the construction of an interference filter, which is composed of two reflective metal layers, separated by one or more layers of dielectric material. White light incident normal to the layers of the filter emerges as an intensity versus wavelength spectrum containing peaks. This spectrum is captured and measured. If the thickness of one or more layers in the filter is changed, a change in the spectrum is induced. Interference theory can be used to determine a change in film thickness from a measured change in the spectrum.[29,30]

Figure 1 shows a schematic of the filter we have used to study the adhesion between metal and mica. It consists of two thin mica sheets, cleaved so their surfaces are molecularly smooth, each coated on one side with a reflective film of either silver or gold. The mica sheets are glued to cylindrical quartz

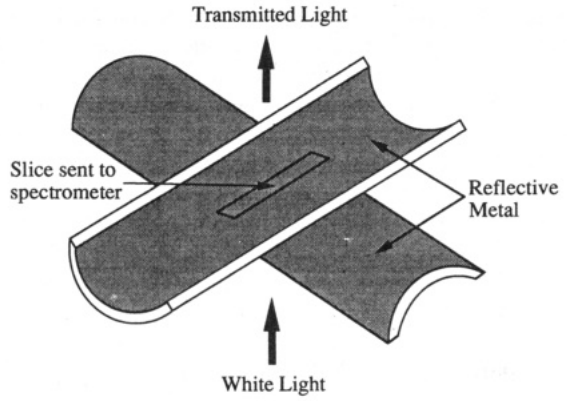

Figure 1. A schematic representation of the crossed-cylinder filter we are using in the SFA. The thin slice of light that is sent to the spectrometer is shown superimposed on the filter.

substrates (radius of curvature 1 cm); one is glued with the bare mica exposed, the other with the metal film exposed. The cylinders are mounted in the SFA at right angles, with the mica surface opposed to the metal surface. The layers in this filter are thus: metal/mica/medium/metal. Although the medium can be any dielectric fluid, in these experiments it was simply dry nitrogen. (Our procedure for preparing the mica sheets and metal films is given in section B.)

A metal/mica interface is created by using the SFA to place the opposed metal and mica surfaces into contact. Generally, when two curved elastic bodies are brought together, they will deform about the region of closest approach.[6,16,31−33] The soft glue holding the mica sheets to their supports undergoes the greatest deformation,[16] leading to a flattened region of metal/mica contact typically tens to hundreds of micrometers in diameter.

In brief, ESA-MBI is used to characterize the roughness of the metal/mica interface by measuring the spectra of light transmitted through the surfaces and comparing it against that transmitted through another, independent filter, where the metal/mica interface is smooth. The two filters will be referred to as the "rough filter" and the "calibration filter", respectively. The rough filter is created with the SFA, as described above; the calibration filter is created by coating a mica sheet, of identical thickness to the mica sheet in the rough filter, on both of its molecularly smooth sides with metal.

The essential difference between the rough filter and the calibration filter is that in the former, dielectric medium is trapped within the metal/mica interface. The presence of dielectric material has an effect on the spectra which can be measured and ultimately used to characterize the degree and form of roughness. Furthermore, since the medium thickness outside of the metal/mica contact region varies with the shape of the deformed surfaces, the deformation of the surfaces can also be characterized. What follows in the rest of this section is a description of how spectra are measured and then analyzed.

One of the great advantages of ESA-MBI is that the spectra transmitted through many small contiguous sections of the filter can be measured simultaneously. A thin slice of the transmitted light, shown superimposed on the filter in Figure 1, is directed into a spectrometer, which acts to disperse the light, or spread it out so that different wavelengths appear at different spatial positions. The intensity versus wavelength spectrum along this slice is captured by a slow-scan charge-coupled device (CCD) camera, mounted at the exit of the spectrometer. The image of the dispersed light is captured by a CCD detector, which is a rectangular grid of square pixels; each pixel measures the intensity of light incident upon it.

The rectangular CCD detector is aligned so its short axis is parallel to the entrance slit of the spectrometer, with its long axis in the dispersion direction. Thus, each row of pixels measures the intensity versus wavelength spectrum transmitted through a section of the filter. The size of this section is set by the width of the entrance slit of the spectrometer, Δs, the height of the pixels, Δx, and the magnification of the emergent light en route to the spectrometer, M. The area of the section is simply $\Delta s \Delta x / M^2$. For our experiments, $\Delta x = 23.2$ μm, $\Delta s = 100$ μm, and $M = 18.2$. Thus, each section is 1.3 μm by 5.5 μm. Instead of the row number, we will use the parameter ϱ to represent the position (in micrometers) of the section of the filter along the slice.

To understand how we interpret and analyze measured spectra, it is first necessary to appreciate, in general terms, how the spectrum of transmitted light is affected by changes in the thickness of the dielectric medium layer, and also by changes in the thickness of the metal layer. If, for example, the metal surface is rough, then both the local metal thickness and the local medium thickness will vary with lateral position across the solid/solid interface. If the surfaces are curved relative to one another (as they are beyond the flattened region of contact), then the thickness of the medium between the surfaces will also vary accordingly. The presence of dielectric material trapped between the metal and mica causes, most predominantly, the peaks in the transmitted spectra to shift to longer wavelengths; the thicker the medium, the greater the shift. On the other hand, variations in thickness of the metal impact markedly the intensity of transmitted light, but have a minor effect on peak wavelengths. What all this means is that the shift in wavelength of the peaks for the rough filter, relative to those for the calibration filter, is a direct reflection of the thickness of the medium layer trapped within the rough filter.[34] Of course, we cannot measure this thickness pointwise but can obtain an average value for each discrete section of the filter that is sampled by the CCD detector.

In handling and interpreting the captured spectral data, it is therefore valuable to characterize each peak by a single number, λ_p, which is an indicator of its location in wavelength space. For example, λ_p could be the wavelength of the center of a peak, or the wavelength of the maximum intensity; some choices are more suitable than others depending on the shapes of peaks transmitted through a filter.[28]

The spectra measured through each section of the filter will generally contain several peaks (corresponding to interference of different orders). As described above, their locations will be different from section to section due to variations in the average thickness of the medium layer from one section to the next. Generally, the medium thickness varies gradually enough that peak locations from one section are not too far removed from those in the adjacent sections. It is thus possible to generate several "peak profiles", each of which is a plot of the location of a peak, λ_p, versus the position of the section, ϱ. It is a great advantage to have multiple peak profiles since structural features in a filter should be mirrored in each profile, and hence small features can be distinguished from noise.

For practitioners of multiple beam interferometry, we note that a peak profile is simply a distillation of the collected spectral data into a set of coordinates, of the form (representative wavelength, position along filter), which characterizes quantitatively a "fringe of equal chromatic order", to use common terminology. Although this could be accomplished by simpler means (such as visually with use of a traveling micrometer, as is often done), our method of data collection permits precise and simultaneous measurements of broad and/or dim fringes,

which are generated when metals besides silver are used in the interference filter.[29] As will be demonstrated herein, such precision is necessary to discern differences between fringes produced by the rough filter and those produced by the calibration filter.

The extent of roughness of the metal/mica interface is characterized by comparing peak profiles for the rough filter with those for the calibration filter. The calibration filter's profile should be flat; i.e., λ_p should be constant for all ϱ (of course, there will be some noise in the peak profile).[28] The rough filter's profile will be shifted to longer wavelength than the calibration filter's, the degree of shift being proportional to the amount of dielectric medium trapped within the metal/mica contact region.

To convert a measured shift to an absolute measure of roughness, it is necessary to invoke a model of the metal topography. Given a chosen model, one varies the extent of roughness until the predicted peak locations match those measured. Clearly, different models yield different values of roughness; however, the extent of this variability can be bracketed. In particular, for a given measured shift the model surface which yields the largest roughness is a "rolling" one, such as a sinusoidal topography, while the model surface which yields the smallest roughness is a "spiked" one, where the metal is smooth except for a few random protrusions of insignificant extent.[34] In other words, to account for a given wavelength shift, the roughness determined from a rolling topographical model (in terms of a peak-to-valley height) will be twice that determined from the spike model (in terms of the height of the spikes).

Hence, assuming any topographical model, estimates of the degree of roughness determined by ESA-MBI are accurate to within a factor of 2. An additional advantage of ESA-MBI, however, is that it can be used to reject certain topographical models as unsuitable; this is because the details of the captured spectra (namely, the shapes of the intensity variations with wavelength) are affected by topography. We have previously shown that the spike model is a suitable one for both silver and gold.[28]

Finally, we emphasize that each point comprising a peak profile is generated from light transmitted though a discrete section of the filter. Thus, through the procedure presented above, one can track section by section the average dielectric content across the filter. Furthermore, if multiple peak profiles are captured on the detector, then multiple estimates of the roughness in each section can be obtained.

B. Measurements of Adhesion Using the SFA. We are using an SFA identical with the one described in detail by others.[14,35] We use the SFA to place the crossed cylinder bodies shown in Figure 1 into contact; one of the cylinders is mounted on a weak leaf spring while the other is attached to a rigid mount. Through a combination of micrometer-driven rods and a piezoelectric crystal, the separation between the surfaces can be varied on a scale ranging from millimeters down to angstroms. If the surfaces are brought together and there are attractive forces acting between them, they can "jump" from a finite separation into contact. The jumps are due to the mechanical instability of the leaf spring that occurs when the gradient of the force acting between the surfaces exceeds the spring constant.[14,35,36]

Once the cylinders have been placed in contact, the SFA can be used to apply controlled external loads to them, either tensile or compressive, by bending the leaf spring. Thus, the deformation of the surfaces can be measured as a function of applied load. The strength of adhesion, or the "pull-off" force, F_p, is measured by applying a slowly increasing tensile load until the surfaces jump apart. The deflection of the spring at the moment of separation is very nearly equal to the separation of the surfaces after the jump,[31] which can be measured using ESA-MBI. F_p is then simply equal to the deflection of the spring multiplied by the spring constant. We used two types of springs in the experiments reported here, a gooseneck cantilever spring (105.5 N/m) and a double cantilever spring (121.5 N/m). Since available theories of adhesion show that F_p/R is constant,[6,33] where R is the radius of the undeformed cylinders, measured values of pull-off force are reported as F_p/R.

III. Preparation and Characterization of Surfaces

Muscovite mica was cleaved into a thin sheet, approximately 3−4 μm, of uniform thickness. Squares of mica (1 cm on a side) were then cut from this sheet and placed on two large support plates of freshly cleaved mica;[37] about half of the mica sheets were on each support plate.

One of the support plates was coated with a metal film (gold or silver), thus covering the exposed faces of the mica sheets, by thermal evaporation from a tungsten boat in a turbo-pumped pyrex bell-jar system. Evaporation rates and final film thicknesses were measured using a quartz crystal monitor. The source metals were 99.999% pure. Base pressure during the evaporation was better than 8×10^{-7} Torr. Rates of evaporation were 2.8 Å/s for gold and between 3.5 and 4.0 Å/s for silver. Film thicknesses were approximately 500 Å. One of the mica sheets was removed from the support plate and glued to a cylindrical quartz disk using the epoxy resin Epon 1004, with the metal side against the resin and the bare mica surface exposed. This cylindrical disk was mounted in the SFA, becoming the upper surface shown schematically in Figure 1.

The lower surface of Figure 1 was prepared by gluing an uncoated mica sheet, from the second support plate, to a quartz disk and then placing it in the evaporation chamber, where a metal film was evaporated onto the mica surface. This coated sheet was then placed in the SFA opposite to the bare mica surface, thus creating the filter shown in Figure 1. The SFA was then sealed up and purged with nitrogen gas for at least 0.5 h before experiments were begun.

Although gold and silver films prepared by evaporation appear mirror-smooth by eye, they are microscopically rough. Fortunately, a great deal is known about the structure of metals, especially gold, evaporated onto mica (a favorite substrate for scanning tunneling microscopy).[38−40] As silver films are employed in Raman spectroscopy, their surface properties are also well established.[41] We used an atomic force microscope (AFM) to profile our silver and gold films in air and obtained the following results (which are in qualitative agreement with the studies just mentioned). The metal films are polycrystalline; silver grains are approximately 20 nm to 30 nm in diameter and gold grains are approximately 10 nm in diameter. The silver surface is dominated by a few tall grains, about 10 per μm^2, which stand taller than the others, typically 5 nm to 75 nm taller. The heights of the grains for the gold films, however, appear more normally distributed about a mean, with an average roughness of approximately 2 nm. We note here that our AFM scans were performed for only one gold and one silver film. Since we did not obtain measurements for many samples, our conclusions should be considered as more qualitative than quantitative.

Modification of Silver Roughness. We previously found that the roughness of an evaporated silver film can be increased by heating it in air to 160 °C for a few minutes.[28] We used an atomic force microscope to image a heated silver surface. The

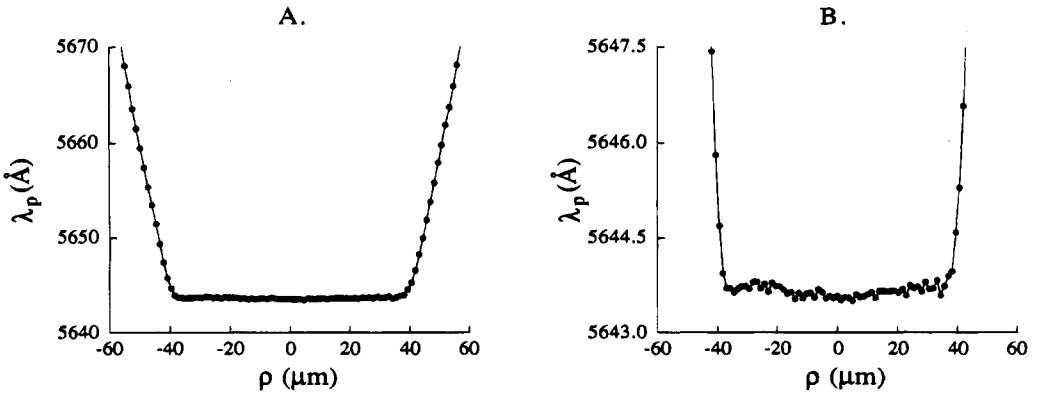

Figure 2. (A) A peak profile for mica/mica contact. (B) A close-up about the flattened contact region.

grains on the surface were about 100 nm in diameter, and the few tall asperities were typically 10 nm to 12 nm above the rest of the silver surface, instead of 5 nm to 7 nm for the unheated surface. This is in reasonable agreement with ESA-MBI measurements[28] that show that silver becomes about twice as rough upon heating over minutes.

In this study, we have prepared silver surfaces of varying roughness by heating them for different periods of time, from 0 min (no heating at all) to approximately 5 min; generally, longer heating times result in rougher surfaces. We note here that since the glue must be heated to approximately 160 °C to mount the mica sheets to their cylindrical supports, the surface preparation procedure described above was followed to avoid unwanted heating of the metals.

IV. Deformation and Adhesion of Two Smooth Mica Surfaces in Contact

Before we describe our measurements for metal/mica contact, we first want to present our measurements of the deformation and adhesion of two smooth mica surfaces in contact. There are three reasons for this. First, an understanding of the behavior of mica/mica contact provides a reference against which the behavior of metal/mica contact can be compared. Second, a careful analysis within the region of mica/mica contact has never been carried out; here we show that ESA-MBI measurements are in qualitative agreement with the predictions of Attard and Parker,[32] who used rigorous elastic theory to calculate the deformations of smooth elastic bodies in contact, taking into account the finite range of surface forces. Third, we believe it is of significant value to establish the reproducibility of measurements obtained with the surface forces apparatus. As measurements of mica/mica contact and adhesion are commonplace in virtually all surface forces laboratories (such measurements are often prerequisites for most experiments), this system is ideal for this purpose.

A typical peak profile is shown in Figure 2A for mica surfaces that were placed into contact under no applied external forces. (A filter similar to the one shown in Figure 1 was used; the only difference is that both metal-coated mica sheets were glued with the bare mica surfaces exposed.) The mica surfaces were driven close to one another until they jumped into contact, and the peak profile was measured immediately after the jump. The deformation of the surfaces, leading to a flattened region of mica/mica contact, is clearly apparent. Note that the boundaries on either side of the flat region are sharp and easy to define. If mica surfaces are left in contact for several hours, virtually no change in the peak profile occurs. The diameter of the contact region may increase slightly, but the wavelength of the flattened region does not change. We previously reported that the glue used to hold the mica sheets to their supports exhibits some viscoelastic behavior,[27] and this may account for the slight increase in the size of the flattened region.

There is some noise in the peak profile, which can be seen by expanding the wavelength scale about the flattened region as in Figure 2B. The level of noise depends on the camera exposure time and the sharpness of the peaks in the measured spectra. The mica sheets in Figure 2 had silver films on their backsides, and the exposure time was 10 s. As a point of reference, the standard deviation in λ_p along the contact region is 0.1 Å. Typically, the noise in λ_p for gold-coated filters is 2 to 3 times greater than for silver-coated filters.

If a compressive load is applied to the mica sheets, the only effect is that the diameter of the flattened region increases with the applied load; the wavelength of the flat region does not change. If the external load is then reduced to zero, the diameter of the contact region shrinks back to the same value before the load was applied. If enough positive force is applied to the mica surfaces, Chen *et al.*[42] have shown that the mica sheets will compress. This would cause a decrease in the wavelength of the flattened part of the peak profile. However, the force must be significant, approximately 50−100 mN, to compress mica enough to create a measurable shift in the peak profile. Finally, if the surfaces are separated and then brought back into contact, the peak profile for subsequent contact is the same as that measured for the first contact.

Our measurements of the force required to pull mica surfaces apart, F_p/R, agree well with those obtained by Christenson, who found that the pull-off force decreases the longer the mica surfaces are exposed to the ambient environment.[43] He suspected, as do we, that the decrease is due to the adsorption of contaminants on the mica surface. In 33 separate experiments, Christenson measured F_p/R for freshly prepared mica and found it to be 1150 ± 260 mN/m. He also found that after 20 h the pull-off force dropped to approximately 75% of its value for freshly prepared mica. In an experiment performed in our laboratory, using freshly prepared mica, we measured a pull-off force of 1380 mN/m. In three other experiments where measurements were made 24 h after preparing the surfaces, F_p/R was 680, 790, and 800 mN/m. For one of those three experiments, F_p/R decreased from 820 mN/m 5 h after preparation to 790 mN/m at 24 h.

One of the distinguishing features between two well-known theories of adhesion is the prediction of the smallest stable diameter of the contact region before separation. One theory, that of Derjaguin, Muller, and Toporov (DMT),[33] predicts the contact area decreases to zero before separation, while the other, that of Johnson, Kendall, and Roberts (JRK),[6] predicts the area decreases to 63% of the diameter at zero applied load. In four separate experiments, we found the diameter of the contact region just prior to separation ranged from 50% to 75% of the

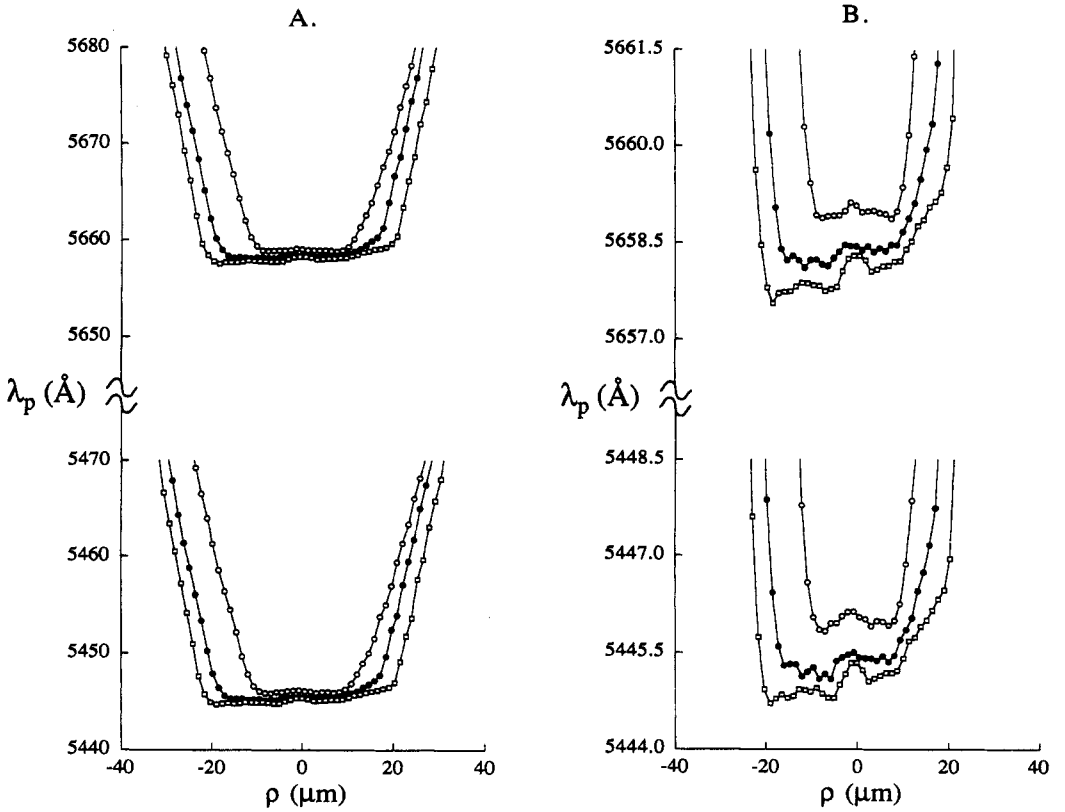

Figure 3. (A) Peak profiles for silver/mica contact at three different times: immediately after contact (open circles), 5 h after contact (filled circles), and 46 h after contact (open squares). (B) Close-ups about the flattened contact region.

diameter measured under zero applied load, with an average of 60%. This is in reasonable agreement with the same measurements made by others[16,44] and with the JKR adhesion theory.

It is particularly interesting to examine the structure and deformations of the mica sheets within the region of contact; we are unaware of any previous attempts to do so. Close-up inspection of the flattened region of the peak profile, Figure 2B, reveals that it is not perfectly flat, as is typically assumed, but there is a very slight downward bow in the center. This feature is real because all the other peak profiles (not shown) reveal the same downward bow in the middle of the contact region. The origin of such a bow is easily rationalized in terms of the non-uniform state of stress existing within the zone of contact. The largest compressive stresses act along the center of contact; at this point the opposed solids are not only at their closest approach (thus exerting the largest repulsive forces on one another), but the elastic bodies are also maximally strained. Both factors would lead to the observed bow in the peak profiles. Although we do not undertake this here, one could ultimately compare our experimental results with the calculations of Attard and Parker;[32] they have shown how the deformation and adhesion of elastic bodies can be determined in a self-consistent manner given knowledge of the range and strength of surface forces acting between them.

V. Deformation and Adhesion of a Rough Metal and Smooth Mica in Contact

The first and most striking observation that can be made regarding contact between a rough metal and smooth mica is that the peak profiles change systematically and irreversibly with time. Figures 3A and 4A illustrate this. Both figures show two adjacent peak profiles in the transmitted spectra, measured at three different times; Figure 3 is for silver/mica contact and Figure 4 is for gold/mica contact. The first peak profiles were measured immediately after the surfaces were brought into contact; we note here that, on approach, the surfaces jumped in. The surfaces were left in contact, under no applied load, and the other peak profiles were taken at later times. As is readily seen, over time the area of deformed metal/mica contact increases and the position of the flattened region, in wavelength space, decreases. If an external load is applied to the surfaces to push them together, this process occurs more rapidly.

These results are consistent with our previous observations of the behavior of silver/mica contact, which we attributed to a time-dependent reduction of the silver roughness.[27] In that previous study, however, we did not use ESA-MBI; instead, we used a translating graticule to visually track the average position, in wavelength, of the flattened parts of the observed interference fringes. The accuracy of this method relied on the generation of sharp fringes, thus restricting the experiments to silver/mica contact. In addition, we had not developed the concept of the calibration filter and were thus unable to characterize quantitatively the changes in roughness. Our results in Figure 4 show that the irreversible behavior previously observed for silver films also occurs for gold.

Although not shown in Figures 3 and 4, the peak profiles of the corresponding calibrations filters are flat and located at smaller wavelengths than those for the rough filters. In this work, we use the spike model to convert the wavelength shifts into an estimate of the roughness. Given the nature of this model, the degree of roughness is expressed in terms of the height of the spikes spanning across the otherwise smooth surfaces or, equivalently, the thickness of the dielectric medium which separates the mica from the metal. As described in section II, a measurement can be obtained for each section (area $\approx 5\ \mu m^2$) of the filter. However, in what follows we report an average value, taken over those sections within the flattened region of mica/metal contact. The uncertainty reported reflects

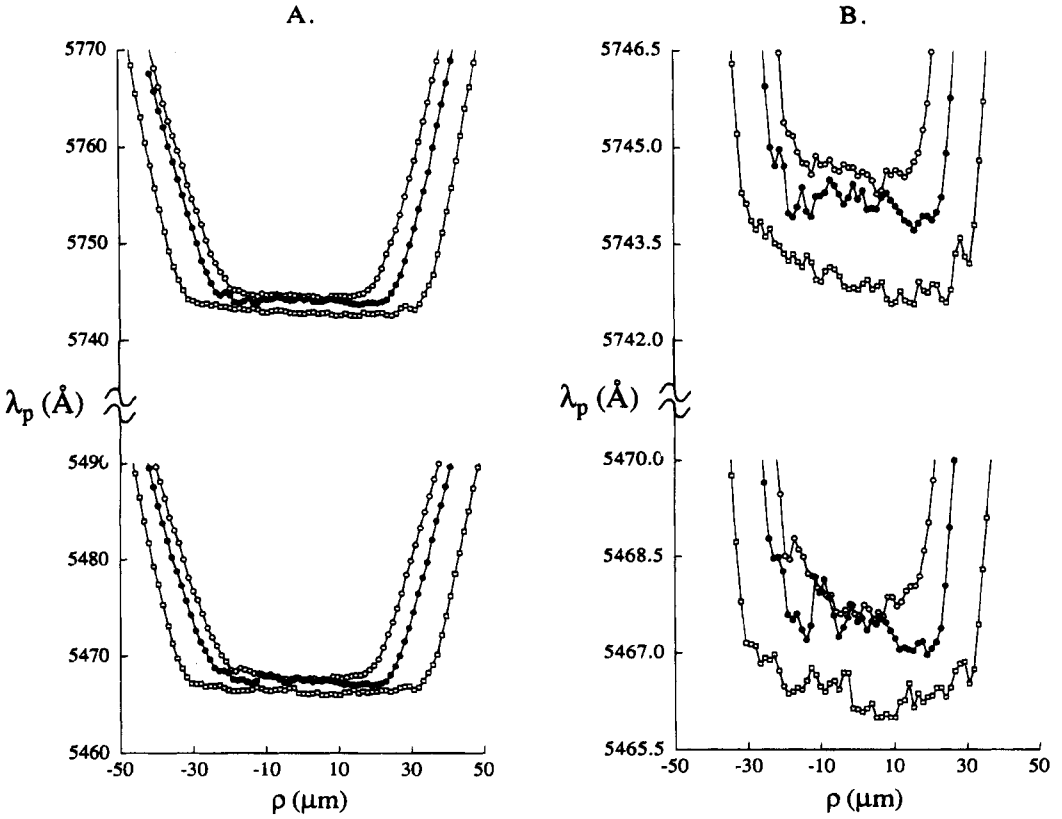

Figure 4. (A) Peak profiles for gold/mica contact at three different times: immediately after contact (open circles), 0.5 h after contact (filled circles), and 19 h after contact (open squares). (B) Close-ups about the flattened contact region.

the measurement error (the origins of which are detailed in ref 28) and also scatter arising from the fact that the region of contact is neither perfectly flat (i.e., of uniform roughness) nor clearly delineated.

In carrying out the analysis, we find that the roughness of the silver/mica interface in Figure 3 is 40 ± 2 Å on initial contact, decreasing to 32 ± 3 Å after 46 h. For the gold/mica contact in Figure 4, initial roughness is 49 ± 4 Å, decreasing to 42 ± 4 Å after 19 h. It is thus clear that metal/mica contact is not perfectly intimate; there is significant dielectric material (in this case air) present between the surfaces. To further verify its presence, one can expose the surfaces to vapors which condense around the region of solid/solid contact. We have done such experiments for metal/mica contact[28] and find that the air trapped within the interface is replaced with condensed liquid; this causes the flattened region of the observed peak profiles to shift to longer wavelength because of the liquid's higher refractive index.

ESA-MBI also allows us to "peer" very closely at the shape of the metal/mica interface. Close inspection of the peak profiles in Figures 3B and 4B shows that the deformed contact region is not as flat as it is for mica/mica contact (Figure 2B). In fact, there are interesting features in the peak profiles that are readily seen. For silver/mica contact, Figure 3B, the contact region becomes progressively more tilted over time, and furthermore there is a slight upward hump in the middle. These features are very similar for both peak profiles, suggesting they arise from real structure and are not due to noise. For gold/mica contact, the peak profiles are noisier; however, they show that the contact region is also slightly tilted. Clearly, the local area averaged deformations experienced by the rough metal surfaces can vary significantly over the nominal region of contact. These results can be contrasted with those for mica/mica contact, where the only structure in the contact region is a very slight downward dip in the center. It is interesting to note that the downward dip is absent at the silver/mica interface, but there is some evidence of a dip at the gold/mica interface. The edge of the metal/mica contact region is difficult to identify, whereas the mica/mica contact region is very sharply defined.

If the mica and metal surfaces are pulled apart and then brought back into contact, the peak profiles for the subsequent contact are different from those measured just before the pulling was started. In Figure 5, peak profiles are shown for gold/mica contact after 18 h (the same one in Figure 4). The surfaces were then pulled apart and brought back into contact, at which point peak profiles were immediately measured; they are also shown in Figure 5. For the subsequent contact, the diameter of the contact region is slightly smaller and the peak profiles are shifted to longer wavelengths. Note especially that the diameter of the contact region is significantly greater than that observed immediately after virgin contact (Figure 4). It appears that the separation process causes the gold to become rougher, although not as rough as the virgin surface. One likely explanation for this is that the gold surface undergoes plastic deformation on separation from mica, behavior previously reported by Gane *et al.*[24] for two gold surfaces. A similar phenomena was reported by McFarlane and Tabor[45] who studied the adhesion of indium to steel. On separating these surfaces from contact, they found that substantial "puckling-up" of the indium had occurred.

Finally, if on subsequent contact the gold and mica surfaces are left together, the same time-dependent behavior is observed where the peak profiles shift to smaller wavelength. This same overall behavior has also been observed for silver/mica contact.

We used the heating procedure described in section III to roughen a silver surface, and found that the deformation of mica and heated silver in contact was dramatically different from that of mica and unheated silver. Figure 6 is a peak profile for contact between mica and the same silver surface from Figure 3 after heating. In contrast to unheated-silver/mica, all the

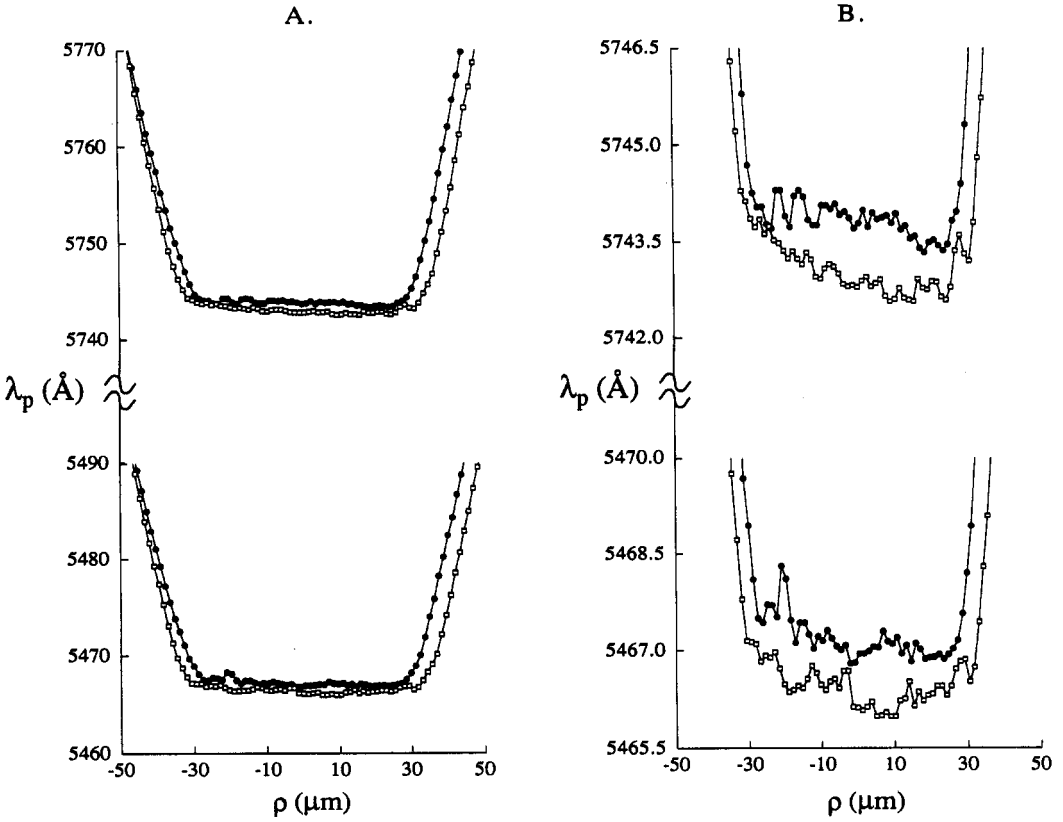

Figure 5. (A) Peak profiles for gold/mica contact after 19 h (open squares); note this is the same profile shown in Figure 4. The surfaces were then separated and brought back into contact; a peak profile was measured immediately after subsequent contact (filled circles). (B) Close-ups about the flattened contact region.

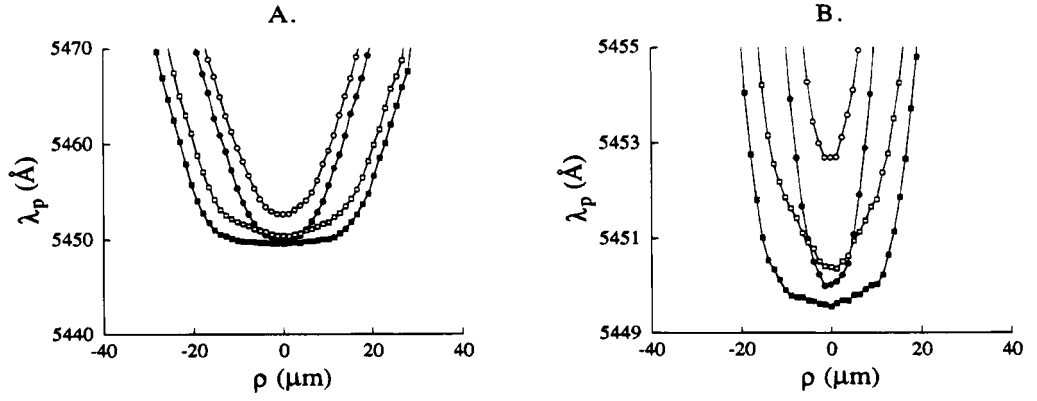

Figure 6. (A) Peak profiles for silver/mica contact after heating the silver in air to 160 °C for 3.5 min. Peak profiles were measured at four different times: immediately after contact (open cirlces), 20 h after contact (filled circles), on application of a 2.5 mN compressive load, also 20 h after contact (open squares), and 38 h after contact, or equivalent, 18 h after the compressive load was applied (filled squares). (B) Close-ups about the flattened contact region.

heated-silver/mica profiles are quite curved about the point of closest approach, and remain that way even after external loads are applied to drive the surfaces together. The profiles do, however, shift over time to shorter wavelengths. The peak profiles shown in Figure 6 were measured at four separate instances; the first was on initial contact, the second after 20 h, the third after a load of 2.5 mN was applied to compress the surfaces (the load was applied immediately after the second profile was measured), and the fourth 18 h after compression. In comparing the profiles to those of the calibration filter, we estimate the roughness of the heated silver to be 105 ± 5 Å on initial contact and 83 ± 5 Å after compression (these values are derived from one only point of the peak profile, namely, that corresponding to the section of the filter at the center of contact).

We wish to report one other interesting difference between the behavior of the unheated and heated silver surfaces. With few exceptions, we found that on bringing an unheated silver film toward the opposing mica sheet, the surfaces jumped into contact from a finite separation. If the silver surface is heated for longer than about 3 to 4 min, however, jumps do not occur on the initial approach into contact, but do occur on all subsequent approaches. Although we do not have a good explanation for this behavior, it does not appear that increased roughness is entirely responsible, since the roughness of the silver is much less than the distance at which jumps occur (approximately 40 nm for the springs used in this study).

So far, we have shown how roughness impacts the deformations and structure of the metal/mica interface. Since ESA-MBI can be incorporated *in situ* with the SFA, we have also

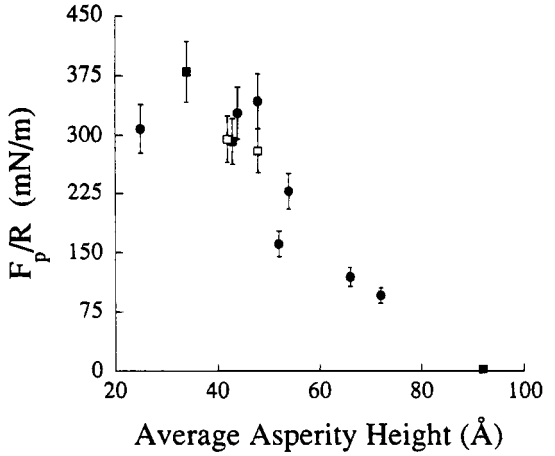

Figure 7. A plot of pull-off force, F_p/R, versus roughness. There are three types of data points, representing: silver/mica where contact was maintained under an applied compressive load of 1 to 7 mN (filled circles), silver/mica where contact was maintained under no applied load (filled squares), and gold/mica where contact was maintained under no applied load (open squares).

been able to measure how roughness impacts the adhesive force, F_p/R. Measurements of F_p/R were made, as a function of roughness, by preparing silver surfaces that had been heated for different lengths of time. However, we found that for surfaces left in contact for short times (less than 10 h), the pull-off forces exhibited significant scatter when plotted versus roughness. The scatter was significantly reduced for those measurements taken after 10 h of contact. We believe this is due to a time-dependent process, whose origin we do not yet understand, which is not directly related to roughness.

In light of these observations, we developed the following protocol to probe directly the influence of roughness on pull-off force. The silver films were placed in contact with mica and were left for over 10 h (the longest was 95 h). In some cases a small compressive load was applied after initial contact, ranging from 1 to 7 mN, and left until separation. Peak profiles were measured at the end of the contact period and then a slowly increasing tensile load (approximately 0.1 mN/s) was applied until the surfaces jumped apart.

Figure 7 is a plot of F_p/R versus roughness determined using the spike model described in section II. Three types of data points are shown in Figure 7; the solid circles represent silver/mica that were in contact under an external load, the solid squares are for silver/mica under no external load, and the open squares are for gold/mica, also under no external load. As is readily seen, the pull-off force decreases steadily with increasing roughness until it becomes effectively zero at about 100 Å.

We were slightly surprised to find that the two measurements of F_p/R for gold/mica contact shown in Figure 7 fall within the silver/mica values. Since these experiments were performed in an ambient environment (where the silver surface was certainly oxidized), it is possible that both surfaces were covered with the same types of airborne contaminants, and thus the reason for similar adhesion forces. We are currently continuing these experiments to assess, among other things, the influence of oxide films and also contaminants on adhesion. It is worthy to note here that in the adhesion study of McFarlane and Tabor[45] strong adhesion was observed even though both the indium and the steel carried appreciable oxide films.

In all experiments performed, we also measured the nominal area of contact just before the surfaces separated. The radius of this contact region was found to range from 40% to 90% of the diameter under zero applied load, with an average of 65%. Of course, as apparent from Figures 3 through 5, the radius of the deformed region for metal/mica contact is not clearly defined, and thus our numbers are estimates. As discussed in section III, this is in reasonable agreement with JKR theory, which predicts the contact area decreases to a nonzero value before separation. There is, however, no reason to expect the JKR theory to apply to the adhesion between nonsmooth surfaces.

As the primary aim of this work was to examine the impact of roughness on adhesion, we compare our results with those of Fuller and Tabor who pressed smooth rubber against a rough surface.[21] In analyzing their experiments, Fuller and Tabor introduced a dimensionless roughness parameter, $\theta = (E\sigma^{3/2})/(r^{1/2}\gamma)$, where E is the elastic modulus, γ is the surface free energy, σ is the average peak height of the rough surface, and r is the radius of curvature of the asperity tips.[4,21] They proposed that if θ is greater than a critical value, the extent of roughness will be such that adhesion is negligible; for their experiments with rubber spheres, they estimated that this critical value was about 10. From our results, where E is about 10^{10} N/m^2 for gold and silver, $\gamma = 0.05$ N/m (the intercept in Figure 7 was estimated to be 500 mN/m and JKR theory was used to convert this to a surface free energy), r is approximately 50 nm (a reasonable estimate from our atomic force microscope images of silver and gold), and $\sigma \approx 100$ Å, we estimate the critical value of θ to be 900. It is, of course, not surprising that our results are not in agreement with predictions from a purely elastic theory. In fact, Fuller and Tabor point out that if the asperities are able to exhibit large extensions before fracture, then the adhesion will be far less susceptible to surface roughness, in accord with our findings.

Evidence for plastic deformations in our metal/mica system includes the time-dependent and irreversible nature of the adhesion process, the dependence of pull-off forces on applied load, and the slight roughening of the metals as they are separated from the mica. Clearly, when any two surfaces are brought together, both elastic and plastic deformations of the contacting asperities may occur. The extent of each depends on the topography of the surface (such as the distribution of asperity heights and curvatures), the material properties of the bulk, and the material properties of the asperities (which may be different from the bulk). Greenwood and Williamson,[46] who put forth a theory of elastic contact between a rough and a smooth surface, developed a simple criterion to estimate the extent of plastic deformations. In particular, they propose that if the "plasticity index", $\Psi = (E/H)\sqrt{(\sigma/r)}$, is greater than one, then the contact is dominated by plastic flow. Here H is the hardness and the other parameters are as defined above. For silver and gold, the hardness is about 10^9 N/m^2; using values for the other parameters as reported above we find $\Psi \approx 5$, a result which is consistent with the direct observations of the adhesion process reported herein.

The experiments reported in this paper can be performed using a variety of metals, besides just silver and gold. Furthermore, the same concepts described in this paper and applied to the study of metal/mica adhesion also apply to metal/metal adhesion, which is especially intriguing since cold-welding can occur.[47] We have used ESA-MBI, in conjunction with the SFA, to observe cold-welding at gold/gold, silver/silver, and gold/silver interfaces.[48] The degree of metal roughness appears to directly control the initiation of this process. Our current work in this area is aimed at further understanding how the mechanical and chemical properties of metals (such as ductility and oxidation state) influence their surface forces and adhesion.

Conclusions

We have used ESA-MBI in conjunction with the SFA to investigate the structure and properties of rough interfaces, as formed between metal and molecularly smooth mica. Upon bringing the metal films into contact with mica, we find that the roughness of the metal film decreases over time, and concurrently the area of flattened metal/mica contact increases. We also measured the adhesion force between mica and metals having different degrees of roughness and found that adhesive forces are not extinguished until the roughness is greater than about 10 nm. The irreversibility of the adhesion process, as well as the variation of adhesive forces with roughness, indicates that the metal film is experiencing significant plastic deformations. Overall, the combination of ESA-MBI with the SFA makes for one of the most powerful, and versatile, techniques for studying solid/solid adhesion.

Acknowledgment. We gratefully acknowledge the support for this work provided by the David and Lucile Packard Foundation, the National Science Foundation Presidential Young Investigator Program (Grant CTS-89-57051), the National Science Foundation MRL Program (Grant DMR91-20668), and a Henkel Corporation Colloid and Surface Science Fellowship awarded to JML.

References and Notes

(1) Kendall, K. *Science* **1994**, *263*, 1720.
(2) *Fundamentals of Adhesion*; Lee, L.-H., Ed.; Plenum Press: New York, 1991.
(3) Israelachvili, J. N. *Intermolecular and Surface Forces*; Academic Press: London, 1985.
(4) Tabor, D. *J. Colloid Interface Sci.* **1977**, *58*, 2.
(5) Johnson, K. L. *Contact Mechanics*; Cambridge University Press: Cambridge, 1985; pp 125−129.
(6) Johnson, K. L.; Kendall, K.; Roberts, A. D. *Proc. R. Soc. London A* **1971**, *324*, 301.
(7) Lee, A. E. *J. Colloid Interface Sci.* **1978**, *64*, 577.
(8) Merrill, W. W.; Pocius, A. V.; Thakker, B. V.; Tirrell, M. *Langmuir* **1991**, *7*, 1975.
(9) Chaudhury, M. K.; Whitesides, G. M. *Langmuir* **1991**, *7*, 1013.
(10) Chaudhury, M. K.; Whitesides, G. M. *Science* **1992**, *255*, 1230.
(11) Chaudhury, M. K.; Owen, M. J. *Langmuir* **1993**, *9*, 29.
(12) Chaudhury, M. K.; Owen, M. J. *J. Phys. Chem.* **1993**, *97*, 5722.
(13) Tabor, D.; Winterton, R. H. S. *Proc. R. Soc. London A* **1969**, *312*, 435.
(14) Israelachvili, J. N.; Adams, G. E. *J. Chem. Soc., Faraday Trans. 1* **1978**, *74*, 975.
(15) Israelachvili, J. N. Ph.D. Thesis, Cambridge University, Cambridge, U.K., 1971.
(16) Horn, R. G.; Israelachvili, J. N.; Pribac, F. *J. Colloid Interface Sci.* **1987**, *115*, 480.
(17) Chen, Y. L.; Helm, C. A.; Israelachvili, J. N. *J. Phys. Chem.* **1991**, *95*, 10736.
(18) Horn, R. G.; Smith, D. T. *Science* **1992**, *256*, 362.
(19) Smith, D. T. *J. Electrostat.* **1991**, *26*, 291.
(20) Horn, R. G.; Smith, D. T.; Grabbe, A. *Nature* **1993**, *366*, 442.
(21) Fuller, K. N. G.; Tabor, D. *Proc. R. Soc. London A* **1975**, *345*, 327.
(22) Briggs, G. A. D.; Briscoe, B. J. *J. Phys. D: Appl. Phys.* **1977**, *10*, 2453.
(23) Tabor, D. In *New Directions in Lubrication, Materials, Wear, and Surface Interactions*; Loomis, W. R., Ed.; Noyes Publications: Park Ridge, NJ, 1985; pp 116−135.
(24) Gane, N.; Pfaelzer, P. F.; Tabor, D. *Proc. R. Soc. London A* **1974**, *340*, 495.
(25) Pethica, J. B.; Tabor, D. *Surf. Sci.* **1979**, *89*, 182.
(26) Thomas, R. C.; Houston, J. E.; Michalske, T. A.; Crooks, R. M. *Science* **1993**, *259*, 1883.
(27) Levins, J. M.; Vanderlick, T. K. *J. Phys. Chem.* **1992**, *96*, 10405.
(28) Levins, J. M.; Vanderlick, T. K. *Langmuir*, submitted for publication.
(29) Levins, J. M.; Vanderlick, T. K. *Langmuir* **1994**, *10*, 2389.
(30) Clarkson, M. T. *J. Phys. D* **1989**, *22*, 475.
(31) Parker, J. L.; Attard, P. *J. Phys. Chem.* **1992**, *96*, 10398.
(32) Attard, P.; Parker, J. L. *Phys. Rev. A* **1992**, *46*, 7959.
(33) Derjaguin, B. V.; Muller, V. M.; Toporov, Y. P. *J. Colloid Interface Sci.* **1975**, *53*, 314.
(34) Levins, J. M.; Vanderlick, T. K. *J. Colloid Interface Sci.* **1993**, *158*, 223.
(35) Vanderlick, T. K.; Scriven, L. E.; Davis, H. T. *Colloids Surf.* **1991**, *52*, 9.
(36) Lodge, K. B.; Mason, R. *Proc. R. Soc. London A* **1982**, *383*, 279.
(37) Israelachvili, J. N. *J. Colloid Interface Sci.* **1973**, *44*, 259.
(38) Buchholz, S.; Fuchs, H.; Rabe, J. P. *J. Vac. Sci. Technol. B* **1991**, *9*, 857.
(39) Chidsey, C. E. D.; Loiacono, D. N.; Sleator, T.; Nakahara, S. *Surf. Sci.* **1988**, *200*, 45.
(40) Golan, Y.; Margulis, L.; Rubinstein, I. *Surf. Sci.* **1992**, *264*, 312.
(41) Van Duyne, R. P.; Hulteen, J. C.; Treichel, D. A. *J. Chem. Phys.* **1993**, *99*, 2102.
(42) Chen, Y. L.; Helm, C. A.; Israelachvili, J. N. *Langmuir* **1991**, *7*, 2694.
(43) Christenson, H. K. *J. Phys. Chem.* **1993**, *97*, 12034.
(44) Israelachvili, J. N. *Faraday Discuss. Chem. Soc.* **1978**, *65*, 20.
(45) McFarlane, J. S.; Tabor, D. *Proc. Roy. Soc. London A* **1950**, *202*, 224.
(46) Greenwood, J. A.; Williamson, J. B. P. *Proc. R. Soc. London A* **1966**, *295*, 300.
(47) Ferguson, G. S.; Chaudhury, M. K.; Sigal, G. B.; Whitesides, G. M. *Science* **1991**, *253*, 776.
(48) Levins, J. M.; Knarr, R. F.; Vanderlick, T. K. To be submitted for publication.

JP942278H